

Original Article

Cite this article: Zheng J, Zong X, Tang L, Guo H, Zhao P, Womer FY, Zhang X, Tang Y, Wang F (2024). Characterizing the distinct imaging phenotypes, clinical behavior, and genetic vulnerability of brain maturational subtypes in mood disorders. *Psychological Medicine* 1–11. <https://doi.org/10.1017/S0033291724000886>

Received: 2 September 2023

Revised: 6 February 2024

Accepted: 15 March 2024

Keywords:

genetic risks; gray matter volume; maturational subtypes; mood disorders; normative modeling

Corresponding author:

Fei Wang;

Email: fei.wang@yale.edu;

Yanqing Tang;

Email: tangyanqing@cmu.edu.cn

Characterizing the distinct imaging phenotypes, clinical behavior, and genetic vulnerability of brain maturational subtypes in mood disorders

Junjie Zheng^{1,2}, Xiaofen Zong³, Lili Tang^{1,2}, Huiling Guo^{1,2,4}, Pengfei Zhao^{1,2}, Fay Y. Womer⁵, Xizhe Zhang⁴, Yanqing Tang^{6,7,8,9} and Fei Wang^{1,2,10} 

¹Early Intervention Unit, Department of Psychiatry, The Affiliated Brain Hospital of Nanjing Medical University, Nanjing, China; ²Functional Brain Imaging Institute of Nanjing Medical University, Nanjing, China; ³Department of Psychiatry, Renmin Hospital of Wuhan University, Wuhan, Hubei, China; ⁴School of Biomedical Engineering and Informatics, Nanjing Medical University, Nanjing, China; ⁵Department of Psychiatry and Behavioral Sciences, Vanderbilt University Medical Center, Nashville, TN, USA; ⁶Department of Psychiatry, The First Hospital of China Medical University, Shenyang, China; ⁷Brain Function Research Section, The First Hospital of China Medical University, Shenyang, China; ⁸Department of Gerontology, The First Hospital of China Medical University, Shenyang, China; ⁹Department of Psychiatry, Shengjing Hospital of China Medical University, Shenyang, China and ¹⁰Department of Mental Health, School of Public Health, Nanjing Medical University, Nanjing, China

Abstract

Background. Mood disorders are characterized by great heterogeneity in clinical manifestation. Uncovering such heterogeneity using neuroimaging-based individual biomarkers, clinical behaviors, and genetic risks, might contribute to elucidating the etiology of these diseases and support precision medicine.

Methods. We recruited 174 drug-naïve and drug-free patients with major depressive disorder and bipolar disorder, as well as 404 healthy controls. T1 MRI imaging data, clinical symptoms, and neurocognitive assessments, and genetics were obtained and analyzed. We applied regional gray matter volumes (GMV) and quantile normative modeling to create maturation curves, and then calculated individual deviations to identify subtypes within the patients using hierarchical clustering. We compared the between-subtype differences in GMV deviations, clinical behaviors, cell-specific transcriptomic associations, and polygenic risk scores. We also validated the GMV deviations based subtyping analysis in a replication cohort.

Results. Two subtypes emerged: subtype 1, characterized by increased GMV deviations in the frontal cortex, cognitive impairment, a higher genetic risk for Alzheimer's disease, and transcriptionally associated with Alzheimer's disease pathways, oligodendrocytes, and endothelial cells; and subtype 2, displaying globally decreased GMV deviations, more severe depressive symptoms, increased genetic vulnerability to major depressive disorder and transcriptionally related to microglia and inhibitory neurons. The distinct patterns of GMV deviations in the frontal, cingulate, and primary motor cortices between subtypes were shown to be replicable.

Conclusions. Our current results provide vital links between MRI-derived phenotypes, spatial transcriptome, genetic vulnerability, and clinical manifestation, and uncover the heterogeneity of mood disorders in biological and behavioral terms.

Introduction

Patients with mood disorders, including bipolar disorder (BD) and major depressive disorder (MDD), exhibit overlapping dominant psychopathology, particularly in the clinical presentation of depressive episodes, which poses ongoing challenges for early diagnosis and intervention (Cassano et al., 2004; Kendler & Gardner, 1998; Krystal, 2014; Kupfer, Frank, & Phillips, 2012; Peralta & Cuesta, 1998). Despite decades of effort, there is still a notable absence of definitive biomarkers for mood disorders. This is not completely surprising because studies have mainly used nosology that differentiates mood disorders according to clinical symptoms in the lack of any objective biomarker, although the clinical diagnostic system, Diagnostic and Statistical Manual of Mental Disorders, has already dramatically revolutionized the psychiatry field. While long proposed as distinguishable diagnostic categories, MDD and BD share substantial key attributes as implicated by complementary sources of evidence from neuroimaging, histological, and genetic studies (Brambilla, Perez, Barale, Schettini, & Soares, 2003; O'Donovan & Owen, 2016; Sheline, 2003; Wei et al., 2020, 2023; Xia et al., 2019). This suggests a broader continuum between MDD and BD than previously assumed. Thus, it is imperative to comprehend the multidimensional neurobiological intermediate phenotypes underlying psychopathology of mood disorders, transcending traditional diagnostic categories for MDD

© The Author(s), 2024. Published by Cambridge University Press. This is an Open Access article, distributed under the terms of the Creative Commons Attribution-NonCommercial-NoDerivatives licence (<http://creativecommons.org/licenses/by-nc-nd/4.0/>), which permits non-commercial re-use, distribution, and reproduction in any medium, provided that no alterations are made and the original article is properly cited. The written permission of Cambridge University Press must be obtained prior to any commercial use and/or adaptation of the article.

and BD. Such understanding is essential for deciphering the diverse pathways that contribute to the heterogeneous clinical symptoms observed across mood disorders.

Recent advancements in characterizing distinct imaging or genetic biotypes have shown promise in revealing biological heterogeneity of mental illness (Marquand, Rezek, Buitelaar, & Beckmann, 2016; Sarrazin *et al.*, 2018; Zhang, Sweeney, Bishop, Gong, & Lui, 2023). Subtyping studies have been advocated as a vital progression toward a more neurologically grounded understanding of heterogeneity in mood disorders (Drysdale *et al.*, 2017; Sun *et al.*, 2023). Numerous investigations have employed various clustering methods to detect neuroimaging-based biotypes in transdiagnostic or diagnosis-specific groups (Chang *et al.*, 2021; Ge, Sassi, Yatham, & Frangou, 2022; Sun *et al.*, 2023). Recent depression studying studies mainly characterizing the distinct emotional symptoms between subgroups (Drysdale *et al.*, 2017; Han *et al.*, 2022). Ge *et al.*, also identified brain maturational subtypes using neuroimaging profiling and characterized the differences in psychopathology and cognition behaviors among youth with mood and anxiety disorders (Ge *et al.*, 2022). Remarkably, they also delineated the biopsychosocial context in which subgroup patients arise (Ge *et al.*, 2022). Distinct neuropathological mechanisms may underlie heterogeneity in the presentation and progression of the clinical phenotype. As we mentioned earlier, assessing the validity of subtyping or clustering results necessitates gathering additional evidence from multidimensional biological data sources that extend beyond clustering algorithm selection and just clinical symptom differences (Chang *et al.*, 2021; Zhang, Wang, & Zhang, 2022). Furthermore, the extent to which genetic heterogeneity influences or interacts with phenotypic expression has barely been explored and individual-level variability, including environment, genetic, or other factors, may lead to different levels of disease liability.

Neuroimaging has yielded a profusion of potential biomarkers for mood disorders (Sheline, 2003). Magnetic resonance imaging studies have revealed the shared and distinct gray matter volume (GMV) reductions in bilateral anterior cingulate and medial frontal cortices, insula in MDD and BD (Drevets, 2000; Jiang *et al.*, 2021). A potential explanation for the intricate findings is the presence of distinct underlying pathophysiology, which resulted in varied patterns of gray matter volume (GMV) abnormalities among different subtypes of patients with mood disorders. Notably, case-control designs, which are supremely prevailing in psychiatry research, yet overlook inter-individual variances that play a critical role in mapping the heterogeneous disease phenotype (Lv *et al.*, 2021). Studies benchmarked each individual scan in the context of normative age-related GMV trends and computed brain charts using individualized centile scores or deviations of neuroanatomical maps (Bethlehem *et al.*, 2022; Chen, Holmes, Zuo, & Dong, 2021). Individual deviations from normative ranges in brain mappings have effectively revealed subgroups of patients with major psychiatric disorders in recent studies (Jiang *et al.*, 2023; Sun *et al.*, 2023). However, the brain morphometric heterogeneity characterized by individual deviations was supposed to have distinct associations with cell-type specific functions and genetic susceptibility in mental illness (Di Biase *et al.*, 2022; Wen *et al.*, 2022), which remain elusive in mood disorders.

Our current study intended to quantify the brain morphological heterogeneity in mood disorders by mapping region-level changes of gray matter volume (GMV) at the level of individual patients. We chart individual GMV deviations utilizing a

normative modeling method that maps inter-individual variances in reference to the healthy control range (Marquand *et al.*, 2019), and use unsupervised clustering method to identify subtypes in patients with MDD and BD. The resulting subtypes were then characterized by using clinical behaviors, cell-specific transcriptomic profiles, and polygenic risk scores (PRS). To minimize the potential influence of medication confounders, we initially conducted our study in a discovery cohort comprising drug-naïve and drug-free patients and then validated the imaging-based subtyping in a replication cohort (Voineskos *et al.*, 2020). It was hypothesized that neuroimaging-based individual deviation biomarkers coupling with multi-dimensional distinct features including clinical behaviors, and genetic risks, can comprehensively describe the underlying heterogeneity in mood disorders.

Methods and materials

Participants

We recruited 114 MDD patients, 60 BD patients and 404 healthy controls (HC). All the patients were recruited from the inpatient department of the Shenyang Mental Health Center and the outpatient clinic of the Department of Psychiatry of the First Affiliated Hospital of China Medical University, Shenyang, China. All the patients were diagnosed by two experienced psychiatrists using the Structured Clinical Interview for the Diagnostic and Statistical Manual of Mental Disorders, 4th Edition, Text Revision (DSM-IV-TR) in patients aged 18 years and older and the Schedule for Affective Disorders and Schizophrenia for School-Age Children-present and Lifetime Version (K-SADS-PL) in those patients under the age of 18 years. The patients were either drug-naïve or had been drug-free for more than two months from oral psychotropic medications before enrollment. The severity of depressive, anxious, and psychopathological symptoms was respectively assessed by using the 17-item Hamilton Depression Rating Scale (HAMD), 14-item the Hamilton Anxiety Rating Scale (HAMA), and Brief Psychiatric Rating Scale (BPRS). We also evaluated participants' cognitive function performance by using Wisconsin Card Sorting Test (WCST). Patients and HC were excluded if they had any major medical condition, neurological disorder, and MRI contraindications (see online Supplementary Material). HC participants were recruited from the local community through advertisement. The participants over 18 years old signed a written consent form themselves. If the participants age were <18 years, their parental/legal guardian provided written informed consent. This study was approved by the Ethics Committee of the First affiliated Hospital of China Medical University (Shenyang, China; Approved number: 2015-27-2). To validate the imaging phenotypes, we involved 268 patients who received medication treatment as the replication cohort. These patients were also recruited and scanned at the First Affiliated Hospital of China Medical University. The details of patients in the replication cohort are described in the online Supplementary Material.

Image acquisition and MRI processing

Structural MRI scanning was conducted on a Signa HDx 3.0 T superconductive MRI system (GE Healthcare, Little Chalfont, UK) at the First Affiliated Hospital, China Medical University. The details of MRI scanning parameters are presented in online

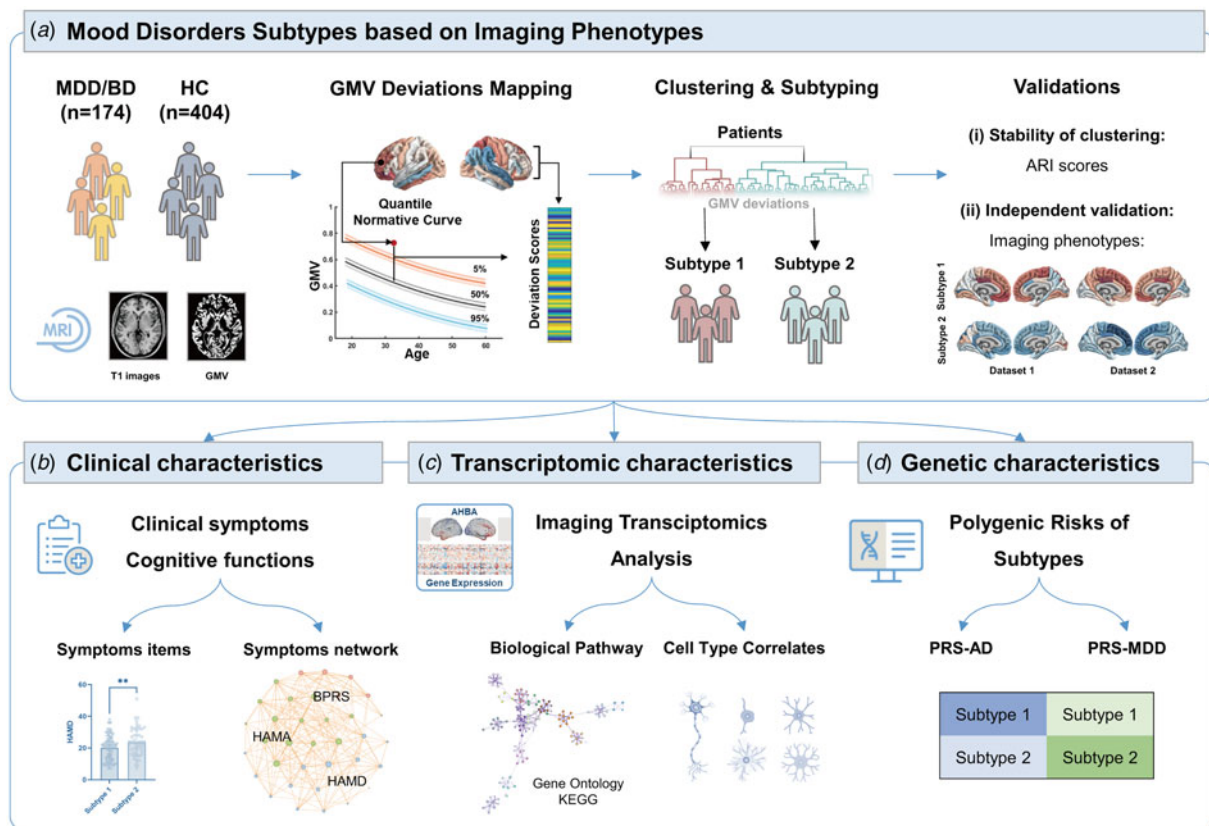


Figure 1. Schematic overview of the workflow in this study. (a) The neuroimaging data were from 174 drug-naïve and drug-free patients with MDD/BD and 404 participants as HC; we used quantile regression model and created normative curves with age based on GMV in HC group and calculated individual deviations for each region; patients were clustered in two subtypes using hierarchical clustering; we then validated the subtyping stability using ARI scores and examined GMV deviations reproducibility in a replication cohort; (b) we compared clinical symptoms and cognitive symptoms differences between subtypes; we also created symptoms network using HAMD, HAMA and BPRS factors and compared global and nodal network properties between subtype groups; (c) we then utilized AHBA brain-wide gene expression data to selected GMV deviations related genes, and identified their biological process and cell type components; and (d) we use PRS-AD and PRS-MD scores to compare AD genetic risk and MDD genetic risk between subtype groups.

Supplementary Material. T1-weighted images were preprocessed by using the Computation Anatomy Toolbox (CAT) implemented in Statistical Parametric Mapping (SPM 12) for voxel-based morphometry (VBM) calculation (<http://www.neuro.uni-jena.de/cat/>) (Gaser & Dahnke, 2016). The quality of images was assessed by using the automated weighted average image quality rating (IQR). We applied the cut-off ($> 80\%$, $\geq \text{grad B}$) to ensure high-quality images for analysis as low-quality images can lead to GM underestimations in preprocessing. Voxel wise gray matter density was calculated and obtained applying CAT12 default parameters. The detailed preprocessing information is presented in online Supplementary Material. The Desikan–Killiany (DK) parcellation atlas partitioned the cortex into 68 cortical regions was used as the regions of interest (ROI) template. ROI-wise gray matter density for each brain region was used for investigating between-group differences.

GMV normative deviation calculation and subtypes clustering

Quantile regression was used to obtain a normative range of regional GMV variation as a function of age and sex described in a previous study (Lv et al., 2021). We positioned individuals with MDD and BD on the normative percentile charts based on HC and expressed three kinds of continuous measurement of

deviation from the generated normative range including the 5th percentile (z_5) quantile regression predictor, the 50th percentile (z_{50}) quantile regression predictor and the 95th percentile (z_{95}) quantile regression predictor, as individual deviation z -scores for each brain region, representing the difference from normative GMV calculated across all HC individuals. We then obtained individual-specific profiles of regional GMV deviations (z_{50} maps) to perform subtyping analysis for all patients. Ward's linkage measurement and hierarchical clustering algorithm were used to identify clusters of patients based on the GMV deviations maps (Fig. 1). We assessed the stability of clustering based on scores of the adjusted rand index (ARI) for 2–5 clusters which were divided by using the hierarchical cutoffs (Hubert & Arabie, 1985). We then chose the clustering solution with the highest averaged ARI following 10-fold cross-validation with 1000 times permutations, as the optimal clustering results. In this study, the 174 drug-free patients constitute the discovery dataset (dataset 1), while the 268 medicated patients comprise the validated dataset (dataset 2). We validate the distinct GMV deviations between subtypes in dataset 1 and assess the correlations of regional deviation findings between dataset 1 and dataset 2.

To further analyze the significantly altered GMV deviations in patients, for each cortical region, we categorized patients as either: (1) within the HC's normative range of variation, labeled as

normal; (2) significantly exceeding the HC's normative range, labeled as supra-normal; or (3) significantly below the HC's normative range, labeled as infra-normal. We used z scores to quantify individual GMV deviation from the 5% and 95%, which was then utilized to guide the above mutually exclusive classification. We acquired the standard deviations for z scores from the bootstrapped confidence intervals (CI). We defined the supra-normal as any individual exceeding the 95% CI for the 95th percentile ($z_{95} > 1.96$), and infra-normal as any individual below the 5% CI for the 5th percentile ($z_5 < -1.96$). Each patient was represented with a GMV deviation encoding map in which brain areas were numerically encoded with either -1 (*infra-normal*), 0 (*normal*), or $+1$ (*supra-normal*), and a GMV deviation z map with matched z_5 or z_{95} values.

The average of the above encoded number across all patients in each subtype group produced a whole-brain summary measurement defined as the average abnormality rate, which quantified the overall percentage of GMV deviation. The average of the GMV deviation z map across all patients in each subtype group defined as the average abnormality extent (mean values of z_{95} or z_5), which quantified the overall extent of GMV deviation.

Clinical information validation in subtype groups

We used two-sample t test to compare the between-subtype differences of clinical measures including total scores of HAMD, HAMA, and BPRS. We also computed the between-group differences in WCST performance among groups. We included five indices of WCST, i.e., correct response (CR), completed categories (CC), total errors (TE), perseverative errors (PE), and non-perseverative errors (NPE). The significant level was set as $p_{FDR} < 0.05$, false discovery rate (FDR) correction – was used for controlling the false positive rate.

We created clinical symptoms network by using correlations between symptoms factors in each subtype and compared the network topological properties based on graph theory (Rydin *et al.*, 2023; Ye *et al.*, 2021). Previous studies suggested psychotic symptoms are considered as the distinct subtype of affective disorders and frequently occur accordingly with depressive and anxious symptoms in all stages of illness (Tonna, De Panfilis, & Marchesi, 2012). In this study, the overall nodes of the symptom network included 17 items of HAMD, 14 items of HAMA, and 5 factors of BPRS (Chang *et al.*, 2021). We conducted paired t tests to examine differences in network strength ranges between subtypes. The details are presented in online Supplementary Materials.

Imaging transcriptomics and virtual histology analysis in subtype groups

Transcriptional data were acquired from the open access Allen Human Brain Atlas (AHBA) database (<https://human.brain-map.org/>). The AHBA dataset was preprocessed according to previous practical guide proposed by Arnatkevic *et al.* (Arnatkeviute, Fulcher, & Fornito, 2019). The five steps of data preprocessing are shown in online Supplementary Materials. Then, we calculated a mean of all tissue samples in a brain area and obtained the matrix (34 regions \times 10 027 genes) of gene expression values. We conducted the multivariate regression approach of partial least squares (PLS) to investigate the transcriptome-imaging associations (Li *et al.*, 2021; Morgan *et al.*, 2019; Romero-Garcia *et al.*, 2020). The details of GMV deviations related to gene expression analysis are presented in

online Supplementary Materials. Then we obtained two PLS1 gene lists respectively for subtype 1 (PLS1-subtype 1) and subtype 2 (PLS1-subtype 2). Finally, we separately performed biological process enrichment for PLS1-subtype 1 and PLS1-subtype 2 using Metascape (<https://metascape.org/>) with false discovery rates correction ($p_{FDR} < 0.05$) (Zhou *et al.*, 2019).

Following the procedure of Seidlitz *et al.* (2020), we obtained corresponding gene sets of seven canonical cell classes (Habib *et al.*, 2017; Lake *et al.*, 2018; Li *et al.*, 2018), including excitatory (Neuro.ex), and inhibitory neurons (Neuro.in), astrocytes (Astro), microglia (Micro), endothelial cells (Endo), oligodendrocyte precursors (OPC), oligodendrocytes (Oligo), and performed virtual histology analysis (Li *et al.*, 2021; Zong *et al.*, 2023). The details of cell-type-specific gene lists selection are presented in online Supplementary Materials. We separately overlapped the gene lists of the seven cell types with the PLS1-subtype 1 and PLS1-subtype 2. First, we tested whether genes of PLS1-subtype 1 and PLS1-subtype 2 significantly overlapped with these cell-type specific genes. The p value of the ratio of overlapped gene number to the cell type gene number was calculated by a permutation test (with $p_{FDR} < 0.05$) (Li *et al.*, 2021). Second, we compared between-subtype differences in the number of overlapped genes of seven cell types with the PLS1-subtype 1 and PLS1-subtype 2, using chi-squared test. The significant level was set as false discovery rates correction $p_{FDR} < 0.05$.

Polygenic risk scores analysis

Details about genotyping and quality control, imputation, and calculation of polygenic risk scores are shown in the online Supplementary Materials. Associations of polygenic risk scores (PRS) including PRS for MDD (PRS-MDD) and PRS for Alzheimer's disease (PRS-AD) were analyzed respectively using logistic regression in both subtype 1 and subtype 2. We calculated Nagelkerke's pseudo- R^2 as a measurement to represent the variance explained by the logistic regression model. We estimated PRS-MDD and PRS-AD at six different levels of p -value thresholds (ranging from $1.0e-06$ to 0.1) in both subtypes 1 and 2 (Euesden, Lewis, & O'reilly, 2015). The significance level of polygenic risks logistic regression model was set as $p_{FDR} < 0.05$.

Results

Clinical and demographic data in the two identified subtypes

The clinical, demographic, and cognitive profiles based on clinical diagnosis of the dataset 1 are shown in online Supplementary Table S1. We used GMV deviations (z_{50} maps) and hierarchical clustering method and identified two subtypes in the MDD and BD samples ($n = 174$), subtype 1 (74 MDD and 38 BD patients), and subtype 2 (40 MDD and 22 BD patients) (online Supplementary Table S2). The clustering stability analysis showed that two clustered subtypes had the highest ARI score among $k = 2-5$ clusters (online Supplementary Figure S3). The distribution of clinical diagnosis (MDD and BD) did not vary between subtype 1 and subtype 2 ($\chi^2 = 0.04$, $p = 0.83$, online Supplementary Table S2). There were no differences in age, gender, or education between subtypes 1 and 2 (online Supplementary Table S2), indicating that the subtype discrimination was not by demographic characteristics. The detailed demographic information of subtypes 1 and 2 identified in the validation cohort are presented in online Supplementary Table S12.

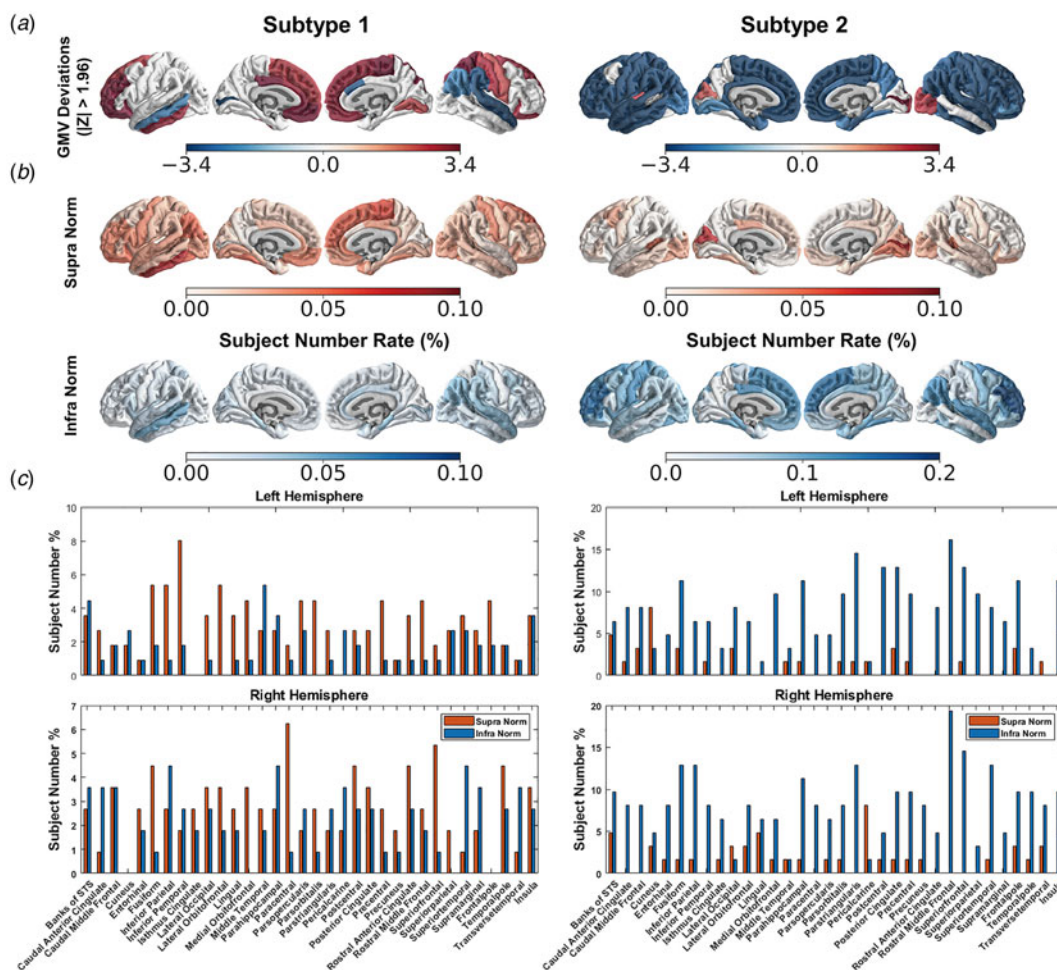


Figure 2. Regions had significant GMV deviations and subject percentages with supra/intra norm regional deviations in subtypes 1 and 2. (a) regions with group mean GMV deviations values $z_{95} > 1.96$ or $z_5 < -1.96$ were presented in both subtypes 1 and subtype 2; (b) we presented the supra and infra GMV deviations individual percentages for each region in both subtypes 1 and 2; (c) the details of supra and infra GMV deviations individual percentages in all regions were presented both subtypes 1 and 2; the red color: supra deviations; the blue color: infra deviations; the color bar: individual percentage.

GMV deviations differences between the two subtypes

In subtype 1, patients showed supra-normal deviations in frontal cortex (orbitofrontal and rostral middle frontal regions, cingulate cortex, and paracentral cortex) and infra-normal deviations in temporoparietal joint area, compared to HC ($z_{95} > 1.96$, $z_5 < -1.96$, $p < 0.05$). In subtype 2, patients showed widespread infra-normal deviations in frontal, temporal, parietal, cingulate cortex, and supra-normal deviation in occipital cortex, compared to HC ($z_{95} > 1.96$, $z_5 < -1.96$, $p < 0.05$) (Fig. 2A). In subtype 1, there were more patients labeled as *supra-normal* in more than half (57.4%) of the brain regions, particularly in prefrontal, cingulate, and paracentral cortex. In contrast, there were more patients labeled as *infra-normal* in subtype 2 in 90% of the cortical regions (Fig. 2B and 2C). The group averaged regional GMV deviations values (z_{50} maps) were mapped and found to show significantly correlations between datasets 1 and 2 in both subtypes 1 ($r = 0.29$, $p < 0.05$) and 2 ($r = 0.45$, $p < 0.0001$) (online Supplementary Fig. S4). The top 10 regions with supra-normal deviations in frontal cortex in subtype 1 and regions with infra-normal deviations in frontal cortex and cingulate cortex in subtype 2 were found consistent in both datasets 1 and 2 (online Supplementary Table S9, Table S10).

Clinical and demographic profiles in the two subtypes

Of the two neuroimaging subtypes we identified, subtype 2 had significantly higher total scores of HAMD than that of subtype 1 ($t = 2.67$, $p_{FDR} = 0.025$, Fig. 3A), while there were no significant between-subtype differences in the total scores of HAMA, BPRS, or illness duration ($p > 0.05$, online Supplementary Table S2). We further explored between-subtype differences in scores for each HAMD item and found that subtype 2 had more prominent guilt ($t = 2.16$, $p = 0.032$), early insomnia ($t = 2.369$, $p = 0.019$), insight ($t = 2.16$, $p = 0.032$), and general somatic symptoms ($t = 2.219$, $p = 0.028$) compared with that of subtype 1 (online Supplementary Fig. S6).

In contrast, as to the between-group comparisons of cognitive function, subtype 1 had poorer performance in the WCST-PE ($t = 4.00$, $p_{FDR} = 0.001$), WCST-NPE ($t = 2.19$, $p_{FDR} = 0.08$), WCST-CR ($t = -3.65$, $p_{FDR} = 0.001$), WCST-CC ($t = -3.63$, $p_{FDR} = 0.001$), and WCST-TE ($t = 3.61$, $p_{FDR} = 0.001$) compared with that of HC, while the WCST performance of subtype 2 did not differ from that of HC (Fig. 3B).

Furthermore, based on graph theory, we created symptom networks for subtypes 1 and 2 using all the items of HAMD, HAMA, BPRS-five factors, and found the global network density and

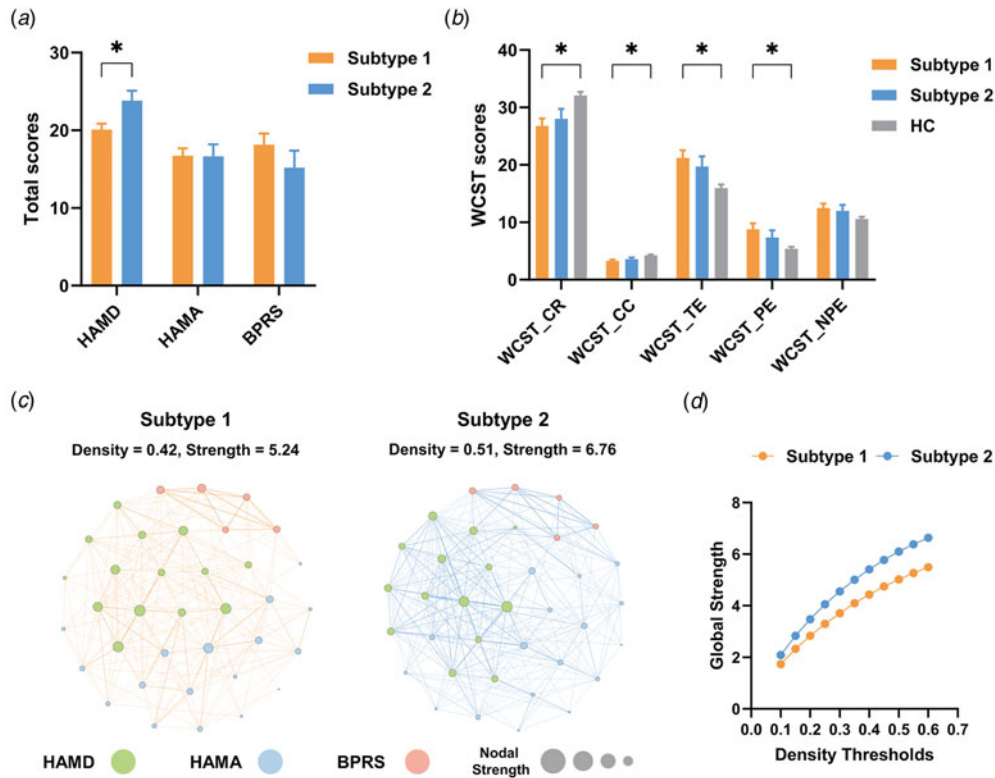


Figure 3. Clinical profiles in the two subtypes. (a) Subtype 2 had significantly higher total scores of HAM-D than that of subtype 1; (b) subtype 1 had poorer WCST performance than that of HC; (c) we created symptom networks for subtype 1 and 2 based on graph theory; (d) subtype 2 had higher network connectivity strength relative to that of subtype 1.

strength were higher in subtype 2 (density = 0.51, strength = 6.76) comparing to that in subtype 1 (density = 0.42, strength = 5.24) (Fig. 3C). Compared with subtype 1, subtype 2 also had higher global network strength under the same network density threshold ($t = 10.17$, $p = 1.0 \times 10^{-6}$, Fig. 3D) and nodal network strength and degree (online Supplementary Fig. S5).

Transcriptomics signatures differences between subtype groups

We utilized a multivariate PLS regression approach to clarify the transcriptional characteristics associated with changes in GMV deviations in subtypes 1 and 2. The PLS1-subtype 1 explained 26.38% of the covariance of GMV deviations across the whole cortex. The PLS1-subtype 1 demonstrated similar spatial gene expression patterns with the deviations map of subtype 1, with positive scores in the frontal, cingulate, precentral cortex, and negative scores in the temporal and occipital cortex (Fig. 4A). Moreover, we detected a significantly positive association between the PLS1-subtype 1 scores and changes of GMV deviations across the whole cortex (PLS1-subtype 1: $r = 0.52$, $p = 0.0017$). The PLS1-subtype 1 was enriched in genes involved in Alzheimer's disease, cell or blood morphogenesis, and cellular component pathways ($p_{FDR} < 0.05$; Fig. 4c, online Supplementary Table S11). The intersection of endothelial cell-related genes with the PLS1-subtype 1 gene list was significantly larger than the intersection of endothelial cell-related genes with the PLS1-subtype 2 gene list. The intersection of oligodendrocytes-related genes with the PLS1-subtype 1 gene list was significantly larger than the intersection of oligodendrocytes-related

genes with the PLS1-subtype 2 gene list. (Fig. 4e, online Supplementary Table S3, S4).

The PLS1-subtype 2 demonstrated similar spatial gene expression patterns with the deviations map of subtype 2, with positive scores in the occipital cortex, and negative scores in the frontal, cingulate, and temporal cortex (Fig. 4b). Moreover, we detected a significantly positive association between the PLS1-subtype 2 scores and changes of GMV deviations across the whole cortex (PLS1-subtype 2: $r = 0.48$, $p = 0.0039$). The PLS1-subtype 2 was enriched in genes involved in ion transport, calcium signaling, trans synaptic signaling, and response to stress biological process ($p_{FDR} < 0.05$; Fig. 4d). The PLS1-subtype 2 genes were significantly enriched in microglia-related genes (the overlapped genes number = 117, permutation $p_{FDR} = 0.005$; Fig. 4F), while marginally enriched in inhibitory neurons-related genes (the overlapped genes number = 157, permutation $p_{FDR} = 0.057$; online Supplementary Table S5).

Genetic risk differences between subtype groups

Four PRS-AD scores at thresholds of p values of 1.0×10^{-6} ($N_{SNPs} = 38$), 1.0×10^{-3} ($N_{SNPs} = 626$), 1.0×10^{-2} ($N_{SNPs} = 3007$), and 0.1 ($N_{SNPs} = 8797$) indicated significant differences between subtype 1 ($n = 19$) and HC ($n = 160$) ($p_{FDR} < 0.05$), explaining 4.2%, 5.9%, 4.1%, and 5.4%, respectively, of the variation in subtype 1. Compared to HC, we observed no significant difference in PRS-AD in subtype 2 ($n = 29$). The PRS-MDD score at thresholds of p values of 1.0×10^{-3} ($N_{SNPs} = 1357$) indicated significant differences between subtype 2 ($n = 29$) and HC ($n = 160$) ($p_{FDR} < 0.05$), explaining 10.8% of the variation in subtype 2. Compared to HC,

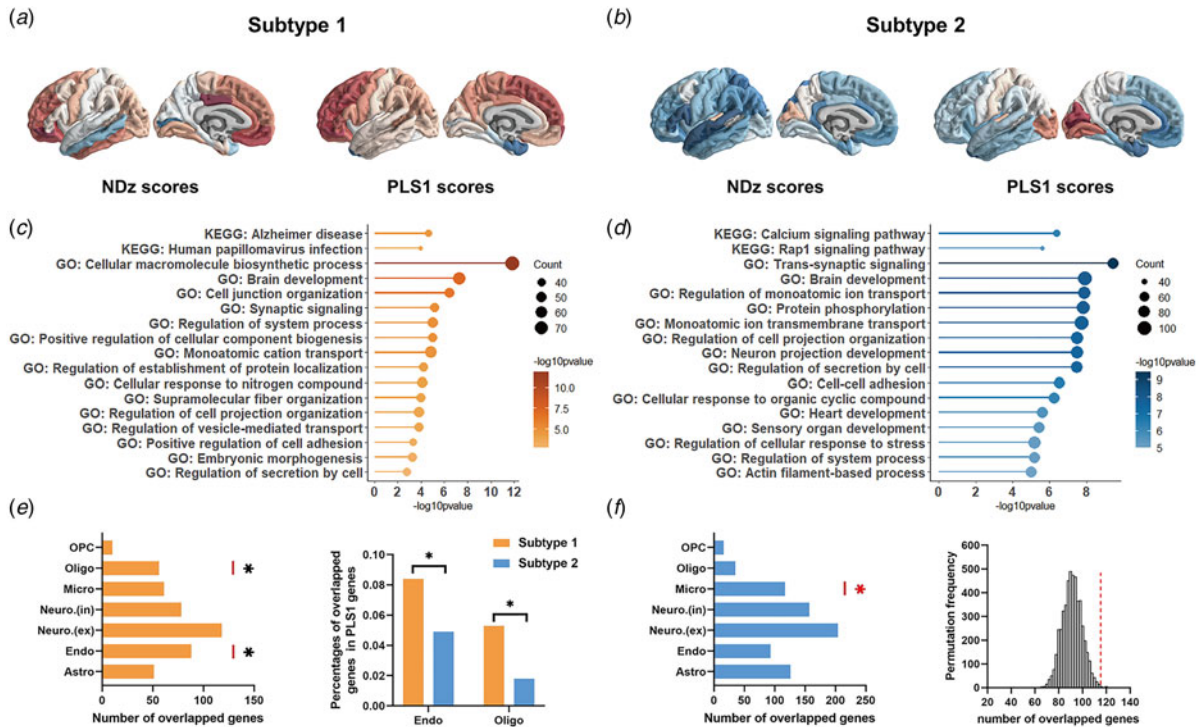


Figure 4. Transcriptomics features and virtual histology of GMV deviations differences in subtypes 1 and 2. (a) Group mean GMV deviations scores in subtype 1 and PLS1-subtype 1 scores in left hemisphere; (b) group mean GMV deviations scores in subtype 2 and PLS1-subtype 2 scores in left hemisphere; (c) top 17 ($p_{FDR} < 0.05$) GO biological process and KEGG pathways enriched using PLS1-subtype 1 genes; (d) top 17 ($p_{FDR} < 0.05$) GO biological process and KEGG pathways enriched using PLS1-subtype 2 genes; (e) the number of overlapped genes between PLS1-subtype 1 genes and cell-specific genes of seven cell types; the black star: significant different between subtypes 1 and 2 using chi-square test at $p_{FDR} < 0.05$; the between-subtype differences of percentages of the overlapped genes in Endo and Oligo; the percentages of overlapped genes mean the number of overlapped genes divide the number of PLS1 genes; the black star: significant different between subtypes 1 and 2 using chi-square test at $p_{FDR} < 0.05$; (f) the number of overlapped genes between PLS1-subtype 1 genes and cell-specific genes of seven cell types; the red star: significant enriched in Micro using permutation test at $p_{FDR} < 0.05$; the distribution of permutation of the number of overlapped genes between random PLS1-subtype 2 genes and micro genes; red dash line present real number of overlapped genes.

there was no significant difference of PRS-MDD in subtype 1. The fitted PRS-AD and PRS-MDD scores for subtypes 1 and 2 are presented in Fig. 5.

Discussion

In this study, we first used a novel hierarchical clustering method based on GMV deviations to identify two subtypes in mood disorders, *supra-normal* (subtype 1) and *infra-normal* (subtype 2) dominant subtypes, which differed in clinical behaviors, cell-specific transcriptomic profiles, and PRS. The *supra-normal* dominant subtype had significantly increased GMV deviations in frontal, cingulate, primary motor cortex, significantly impaired cognitive function (executive function) in the WCST performance, and significantly higher genetic risk for Alzheimer’s disease. Furthermore, the genes of which transcriptional levels showed spatial associations with variations of GMV deviations in the *supra-normal* subtype enriched in Alzheimer’s disease pathways, as well as biological processes such as cell, blood morphogenesis, and cellular component. In addition, the *supra-normal* subtype-related genes were significantly enriched in endothelial cells. In contrast, *infra-normal* dominant subtype demonstrated significantly decreased GMV deviations in frontal, temporal, parietal, and cingulate cortex, significantly severe depressive symptoms, and significantly higher genetic vulnerability to MDD. The genes from the spatial correlation and virtual histology analyses of *infra-normal* subtype significantly enriched in ion

transport, calcium signaling, trans synaptic signaling, and response to stress biological process and inhibitory neurons. Collectively, our findings indicated opposite brain developmental patterns as a core and distinctive characteristic across the mood disorder continuum. Furthermore, the *supra-normal* and *infra-normal* dominant subtypes, delineated by this feature exhibited distinct associations with clinical behaviors, cell-specific transcriptomic profiles, and genetic risks. These imaging phenotypes between subtypes replicated in an independent dataset. Our current results provide insight into the heterogeneity of mood disorders in biological and behavioral terms and indicate a potential advancement toward categorical subtyping and, potentially, the development of precise individualized treatment for patients with MDD and BD.

A primary finding from this study is the identification of the *supra-normal* dominant subtype that had significantly increased GMV deviations in frontal cortex. Although the reasons for this abnormality are currently uncertain, one potential explanation for this phenomenon is that it may be associated with an inflammatory response usually occurred in the early phase of mood disorder (Chen et al., 2023; Gritti, Delvecchio, Ferro, Bressi, & Brambilla, 2021; Qiu et al., 2014). In the initial stage of inflammation, it is known that endothelial cells, regulating inflammation through the expression of adhesion molecules and the release of cytokines and chemokines (Poher & Sessa, 2015), can activate leukocytes and promote their recruitment to sites of inflammation, which could increase cortical morphology (Kaplanski, 2018).

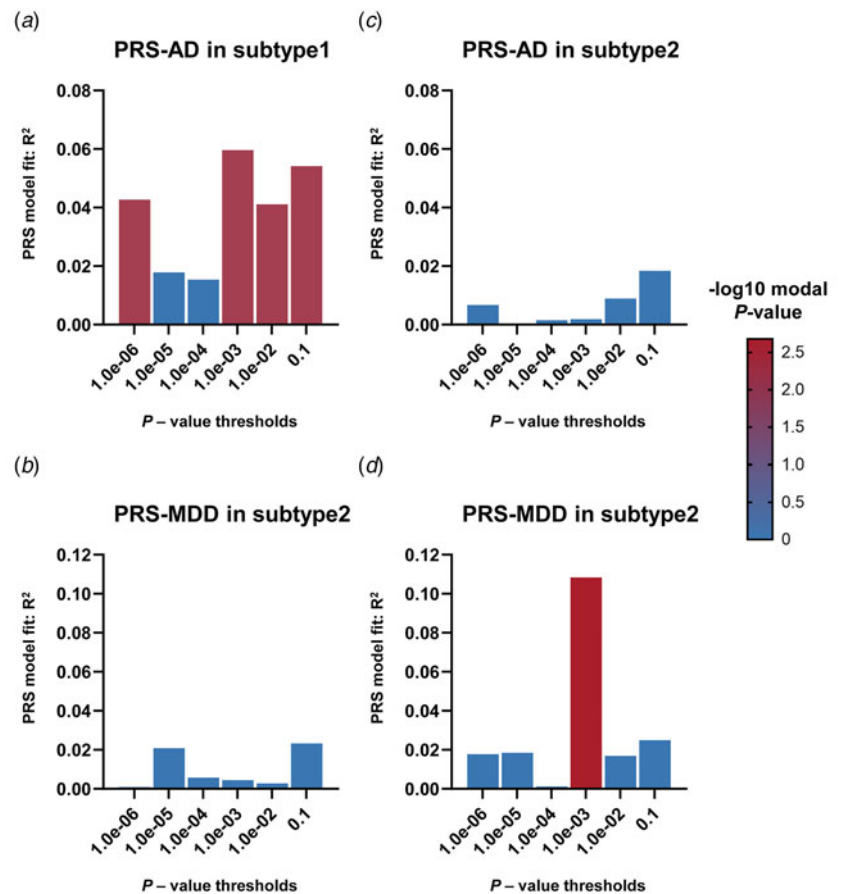


Figure 5. PRS-AD and PRS-MDD scores in subtypes 1 and 2. (a) PRS-AD model were significantly fitted in subtype 1 at SNP threshold $p < 1.0e-06$, $p < 1.0e-03$, $p < 1.0e-02$, $p < 1.0e-01$, while PRS-AD model was not fitted in subtype 2; (b) PRS-MDD model were significantly fitted in subtype 2 at SNP threshold $p < 1.0e-03$, while PRS-MDD model was not fitted in subtype1; red bar presents the PRS-AD or PRS-MDD fit model had a significant level of $p_{FDR} < 0.05$.

Interestingly, our current study revealed that the variations of GMV deviations in the supra-normal subtype were spatially associated with the transcriptional levels of genes, which were mainly enriched in endothelial and oligodendrocytes cells as well as Alzheimer disease pathways. There is growing evidence suggesting that both oligodendrocytes and endothelial cells play important roles in cognitive function and Alzheimer's disease (Desai *et al.*, 2010). Oligodendrocytes are responsible for myelination of axons, which is essential for proper neuronal communication and plasticity (Fields, 2015; Frühbeis *et al.*, 2013). Recent studies have demonstrated that disruptions in oligodendrocyte function and myelination can lead to cognitive impairments (Henn *et al.*, 2022). Similarly, endothelial cells play a crucial role in maintaining the integrity of the blood-brain barrier (BBB), which is important for regulating the exchange of substances between the blood and the brain (Zlokovic, 2011). Dysfunction of the BBB has been associated with various neurological disorders and has been implicated in the pathogenesis of neurocognitive disorders such as Alzheimer's disease (Sweeney, Sagare, & Zlokovic, 2018). More importantly, the validation findings, presented in turn, demonstrated that patients in this *supra-normal* subtype had significantly higher genetic risk for Alzheimer's disease. These findings potentially explain that depression with cognitive impairment leading to a 'pseudodementia' presentation may serve as risk factor of Alzheimer's disease (Byers & Yaffe, 2011; Green *et al.*, 2003; Kessing & Andersen, 2004). Consistently, as to the between-group comparisons of cognitive function, this subtype had poorer performance in the executive cognition functions such as WCST.

In contrast, subtype 2 showed evidence of infra-normal development pattern involving almost globally lower GMV deviations. Our findings can be considered as potential evidence of developmental abnormalities in packing density and cell size which resonates with anomalies in cerebral maturation observed in neurodevelopmental disorders (Ge *et al.*, 2022). In addition, the PLS1-subtype 2 genes were enriched in biological processes such as trans-synaptic signaling and regulation of cellular response to stress, and the genes from the virtual histology analyses of this subtype significantly enriched in microglia and inhibitory neurons, the most abundant neurons in GABAergic system. Microglia are key immune cells in the brain that play a role in regulating synaptic pruning and neuroinflammation (Inta, Lang, Borgwardt, Meyer-Lindenberg, & Gass, 2017). Recent studies have suggested that dysregulation of microglial function may contribute to the development of depressive symptoms (Calcia *et al.*, 2016). In addition, inhibitory neurons, which utilize the neurotransmitter GABA, are crucial in modulating the excitatory activity of neural circuits involved in mood regulation (Brambilla *et al.*, 2003; Croarkin, Levinson, & Daskalakis, 2011; Kalueff & Nutt, 2007). Dysregulation of GABAergic signaling has also been implicated in the pathophysiology of depression. Together, dysfunction of microglia, inhibitory neurons, and GABAergic signaling may contribute to the development of depressive symptoms. Consistently, our validation of PRS analysis demonstrated that patients in this subtype had significantly higher genetic risk for MDD. Of more importance, this subtype had higher total scores of depression severity than subtype 1. As to the comparison of each HAMD sub-item, subtype 2 had more prominent guilt, early insomnia, insight,

and general somatic symptoms. These findings indicated that our neuroimaging subtype delineation not only separates mildly and severely ill patients with mood disorder, but also identifies their subitem heterogeneity regarding guilt, early insomnia, general somatic, and insight features, which have long been considered in mood disorder research (Peralta & Cuesta, 1998; Peterson & Benca, 2006; Zhao et al., 2018). In addition, the symptom network analysis revealed that patients in subtype 2 had a higher network connectivity strength than subtype 1. The greater symptom network strength may reflect a pattern of denser symptom interactions possibly owing to the globally lower GMV deviations in the infra-normal patients. Findings in this study advance the clinical conceptualization by relating them to diverse regional changes in structural brain systems.

Mood disorders are heterogeneous diseases genetically, neurobiologically, and clinically, posing a considerable challenge for treatment and management of patients. Although current development of medication has paid attention to the complex clinical syndromes, advances in psychopharmacology for mood disorders have been restricted for decades. It may be important for nosology and treatment development that neurobiological and genetic heterogeneity in these syndromes would be further elucidated to establish targeted interventions for discrete subtypes similar to many fields in medicine. Our findings indicate a move forward in that direction. Although there has been a growing interest in the heterogeneity of mood disorders in recent years, most previous work has addressed this issue by sorting patients separately according to their behavioral, imaging, or genetic features. This approach may limit our ability to delineate the degree to which genetic heterogeneity impacts or interacts with neuroimaging and behavioral phenotypes. Interestingly, imaging transcriptomics analysis promoted the heuristic attempts and findings of cognitive impairment subtypes may have a genetic risk of AD and subtypes with more severe depressive symptoms may have genetic vulnerability to MDD. Uniting neuroimaging with data from genetics as well as clinical data and integrative computational strategies would enable imaging phenotypes subtyping to traverse the knowledge gap between genetic heterogeneity and clinical observations (Brennan, Landek-Salgado, & Sawa, 2014; Krystal, 2014). Thus, establishing multi-dimensional characteristics of biological heterogeneity may provide a more prospective approach for subtype identification in terms of treatment development and clinical utility.

Studies that use trans-diagnostic methods are emerging as converging evidence implicated core features across mood disorders, with an increasing focus on the neuroimaging biomarkers and genetic risks from a systems perspective. Our current findings defined two distinctive subtypes across traditional clinical diagnostic boundaries. In each subtype reported herein, both MDD and BD were represented. The mismatch between clinical diagnoses and subtypes may partially explain frequent inconsistent findings among previous studies according to clinical diagnosis. The constraints of present diagnostic framework are apparent (Clementz et al., 2016; Ivleva et al., 2017; Meda et al., 2016; Pearlson, Clementz, Sweeney, Keshavan, & Tamminga, 2016). Refining the present diagnostic system with corresponding objective biological measures (e.g. supra-normal and infra-normal GMV) would generate more biologically homogeneous categories, which play a critical role in the development of more personalized and effective treatments.

There are several limitations to this work. First, the use of gene expression profiles from the healthy human brain in AHBA to explain GMV deviations changes is limited to the extent that transcription in patients could be different from those in healthy

brains. Additionally, the AHBA gene expression data including the right hemisphere of the brain for only two participants, restricts the representation of the spatial correlation between entire brain transcriptional level and GMV deviations. Future studies need to incorporate more extensive datasets to comprehensively explore imaging transcriptomic relationships. Second, the genetic data size in our study was small. Future work with a larger sample size of genetic data is desirable. Third, we only used WSCT scores to test cognitive functions between subtype groups. Some other cognitive batteries would be validated in future work. Fourth, we did not obtain specific data about illness severity of the first episode in medication-free patients and were not able to detect the associations between GMV alterations and prior depressive/anxious/psychotic symptoms.

In this study, mood disorders were characterized into two subtypes associated with brain morphology, behavioral phenotypes, and genetic risk profiles. Our findings provide vital links between MRI-derived phenotypes, spatial transcriptome, and genetic vulnerability, illustrating the feasibility of integrating multi-omics information across multi-dimensional biological scales. The identification and validation of the two subtypes provide a potential framework for future studies about the underlying neuropathological mechanisms and genetic heterogeneity as well as precise clinical care in mood disorders.

Supplementary material. The supplementary material for this article can be found at <https://doi.org/10.1017/S0033291724000886>.

Data and code availability. Human gene expression data that support the findings of this study are available in the Allen Brain Atlas ('Complete normalized microarray datasets', <https://human.brainmap.org/static/download>). The code for gene expression preprocessing can be found in previous study and can be downloaded at <https://github.com/BMHLab/AHBAprocessing>. The probe-to-gene annotations were obtained by the Re-annotator toolkit (v1.0.0, <https://sourceforge.net/projects/reannotator/>). All data supporting the findings of this study are provided within the paper and its supplementary information. Additional datasets are available from the corresponding author upon request. All the brain imaging, clinical behavior, and genetic results and the analysis codes in this study are available at https://github.com/zhengjunjie1234/Mood_Disorders_subtypeing.git.

Acknowledgements. This study was supported by grants from National Science Fund for Distinguished Young Scholars (81725005), National Natural Science Foundation of China-Guangdong Joint Fund (NSFC-Guangdong Joint Fund) (U20A6005), National Natural Science Foundation of China (62176129), National Key Research and Development Program (2022YFC2405603) and China Postdoctoral Science Foundation (2022M721681).

Author contributions. Authors Junjie Zheng, Lili Tang, Huiling Guo, Pengfei Zhao, Xizhe Zhang, Yanqing Tang, and Fei Wang were involved in participants recruitment and data collection. Junjie Zheng and Lili Tang executed the neuroimaging and multi-omic analysis. Junjie Zheng, Fay Y. Womer, Fei Wang, and Xiaofen Zong wrote the first draft of the manuscript. Yanqing Tang and Fei Wang guided the study design. Fei Wang supervised the whole study and revised the manuscript. All the authors contributed to the final version of the paper.

Competing interests. The authors report no biomedical financial interests or potential conflicts of interest.

References

- Arnatkeviciute, A., Fulcher, B. D., & Fornito, A. (2019). A practical guide to linking brain-wide gene expression and neuroimaging data. *NeuroImage*, 189, 353–367. doi:10.1016/j.neuroimage.2019.01.011

- Bethlehem, R. A., Seidlitz, J., White, S. R., Vogel, J. W., Anderson, K. M., Adamson, C., ... Areces-Gonzalez, A. (2022). Brain charts for the human lifespan. *Nature*, *604*(7906), 525–533. doi:10.1038/s41586-022-04554-y
- Brambilla, P., Perez, J., Barale, F., Schettini, G., & Soares, J. (2003). GABAergic dysfunction in mood disorders. *Molecular Psychiatry*, *8*(8), 721–737. doi:10.1038/sj.mp.4001362
- Brennan, K. J., Landek-Salgado, M. A., & Sawa, A. (2014). Modeling heterogeneous patients with a clinical diagnosis of schizophrenia with induced pluripotent stem cells. *Biological Psychiatry*, *75*(12), 936–944. doi:10.1016/j.biopsych.2013.10.025
- Byers, A. L., & Yaffe, K. (2011). Depression and risk of developing dementia. *Nature Reviews Neurology*, *7*(6), 323–331. doi:10.1038/nrneuro.2011.60
- Calcia, M. A., Bonsall, D. R., Bloomfield, P. S., Selvaraj, S., Barichello, T., & Howes, O. D. (2016). Stress and neuroinflammation: A systematic review of the effects of stress on microglia and the implications for mental illness. *Psychopharmacology*, *233*, 1637–1650. doi:10.1007/s00213-016-4218-9
- Cassano, G. B., Rucci, P., Frank, E., Fagioli, A., Dell'Osso, L., Shear, M. K., & Kupfer, D. J. (2004). The mood spectrum in unipolar and bipolar disorder: Arguments for a unitary approach. *American Journal of Psychiatry*, *161*(7), 1264–1269. doi:10.1176/appi.ajp.161.7.1264
- Chang, M., Womer, F. Y., Gong, X., Chen, X., Tang, L., Feng, R., ... Zhang, R. (2021). Identifying and validating subtypes within major psychiatric disorders based on frontal-posterior functional imbalance via deep learning. *Molecular Psychiatry*, *26*(7), 2991–3002. doi:10.1038/s41380-020-00938-6
- Chen, L.-Z., Holmes, A. J., Zuo, X.-N., & Dong, Q. (2021). Neuroimaging brain growth charts: A road to mental health. *Psychoradiology*, *1*(4), 272–286. doi:10.1093/psyrad/kkab022
- Chen, M.-H., Hsu, J.-W., Huang, K.-L., Tsai, S.-J., Tu, P.-C., & Bai, Y.-M. (2023). Inflammatory cytokines in and cognitive function of adolescents with first-episode schizophrenia, bipolar disorder, or major depressive disorder. *CNS Spectrums*, *28*(1), 70–77. doi:10.1017/S1092852921000857
- Clementz, B. A., Sweeney, J. A., Hamm, J. P., Ivleva, E. I., Ethridge, L. E., Pearlson, G. D., ... Tamminga, C. A. (2016). Identification of distinct psychosis biotypes using brain-based biomarkers. *American Journal of Psychiatry*, *173*(4), 373–384. doi:10.1176/appi.ajp.2015.14091200
- Croarkin, P. E., Levinson, A. J., & Daskalakis, Z. J. (2011). Evidence for GABAergic inhibitory deficits in major depressive disorder. *Neuroscience & Biobehavioral Reviews*, *35*(3), 818–825. doi:10.1016/j.neubiorev.2010.10.002
- Desai, M. K., Mastrangelo, M. A., Ryan, D. A., Sudol, K. L., Narrow, W. C., & Bowers, W. J. (2010). Early oligodendrocyte/myelin pathology in Alzheimer's disease mice constitutes a novel therapeutic target. *The American Journal of Pathology*, *177*(3), 1422–1435. doi:10.2353/ajpath.2010.100087
- Di Biase, M. A., Geaghan, M. P., Reay, W. R., Seidlitz, J., Weickert, C. S., Pebay, A., ... Zalesky, A. (2022). Cell type-specific manifestations of cortical thickness heterogeneity in schizophrenia. *Molecular Psychiatry*, *27*(4), 2052–2060. doi:10.1038/s41380-022-01460-7
- Drevets, W. C. (2000). Neuroimaging studies of mood disorders. *Biological Psychiatry*, *48*(8), 813–829. doi:10.1016/s0006-3223(00)01020-9
- Drysdale, A. T., Grosenick, L., Downar, J., Dunlop, K., Mansouri, F., Meng, Y., ... Etkin, A. (2017). Resting-state connectivity biomarkers define neurophysiological subtypes of depression. *Nature Medicine*, *23*(1), 28–38. doi:10.1038/nm.4246
- Euesden, J., Lewis, C. M., & O'reilly, P. F. (2015). PRSice: Polygenic risk score software. *Bioinformatics (Oxford, England)*, *31*(9), 1466–1468. doi:10.1093/bioinformatics/btu848
- Fields, R. D. (2015). A new mechanism of nervous system plasticity: Activity-dependent myelination. *Nature Reviews Neuroscience*, *16*(12), 756–767. doi:10.1038/nrn4023
- Frühbeis, C., Fröhlich, D., Kuo, W. P., Amphornrat, J., Thilemann, S., Saab, A. S., ... Nave, K.-A. (2013). Neurotransmitter-triggered transfer of exosomes mediates oligodendrocyte–neuron communication. *PLoS Biology*, *11*(7), e1001604. doi:10.1371/journal.pbio.1001604
- Gaser, C., & Dahnke, R. (2016). CAT—A computational anatomy toolbox for the analysis of structural MRI data. Preprint at www.biorxiv.org/content/10.1101/2022.06.11.495736v2.full
- Ge, R., Sassi, R., Yatham, L. N., & Frangou, S. (2022). Neuroimaging profiling identifies distinct brain maturational subtypes of youth with mood and anxiety disorders. *Molecular Psychiatry*, *28*(3), 1072–1078. doi:10.1038/s41380-022-01925-9
- Green, R. C., Cupples, L. A., Kurz, A., Auerbach, S., Go, R., Sadovnick, D., ... Edeki, T. (2003). Depression as a risk factor for Alzheimer disease: The MIRAGE Study. *Archives of Neurology*, *60*(5), 753–759. doi:10.1001/archneur.60.5.753
- Gritti, D., Delvecchio, G., Ferro, A., Bressi, C., & Brambilla, P. (2021). Neuroinflammation in major depressive disorder: A review of PET imaging studies examining the 18-kDa translocator protein. *Journal of Affective Disorders*, *292*, 642–651. doi:10.1016/j.jad.2021.06.001
- Habib, N., Avraham-Davidi, I., Basu, A., Burks, T., Shekhar, K., Hofree, M., ... Regev, A. (2017). Massively parallel single-nucleus RNA-seq with DroNc-seq. *Nature Methods*, *14*(10), 955–958. doi:10.1038/nmeth.4407
- Han, S., Zheng, R., Li, S., Zhou, B., Jiang, Y., Fang, K., ... Zhang, Y. (2022). Resolving heterogeneity in depression using individualized structural covariance network analysis. *Psychological Medicine*, *53*(11), 1–10. doi:10.1017/S0033291722002380
- Henn, R. E., Noureldein, M. H., Elzinga, S. E., Kim, B., Savelieff, M. G., & Feldman, E. L. (2022). Glial-neuron crosstalk in health and disease: A focus on metabolism, obesity, and cognitive impairment. *Neurobiology of Disease*, *170*, 105766. doi:10.1016/j.nbd.2022.105766
- Hubert, L., & Arabie, P. (1985). Comparing partitions. *Journal of Classification*, *2*, 193–218. doi:10.1007/BF01908075
- Inta, D., Lang, U. E., Borgwardt, S., Meyer-Lindenberg, A., & Gass, P. (2017). Microglia activation and schizophrenia: Lessons from the effects of minocycline on postnatal neurogenesis, neuronal survival and synaptic pruning. *Schizophrenia Bulletin*, *43*(3), 493–496. doi:10.1093/schbul/sbw088
- Ivleva, E. I., Clementz, B. A., Dutcher, A. M., Arnold, S. J., Jeon-Slaughter, H., Aslan, S., ... Meda, S. A. (2017). Brain structure biomarkers in the psychosis biotypes: Findings from the bipolar-schizophrenia network for intermediate phenotypes. *Biological Psychiatry*, *82*(1), 26–39. doi:10.1016/j.biopsych.2016.08.030
- Jiang, X., Wang, X., Jia, L., Sun, T., Kang, J., Zhou, Y., ... Tang, Y. (2021). Structural and functional alterations in untreated patients with major depressive disorder and bipolar disorder experiencing first depressive episode: A magnetic resonance imaging study combined with follow-up. *Journal of Affective Disorders*, *279*, 324–333. doi:10.1016/j.jad.2020.09.133
- Jiang, Y., Wang, J., Zhou, E., Palaniyappan, L., Luo, C., Ji, G., ... Huang, C.-C. (2023). Neuroimaging biomarkers define neurophysiological subtypes with distinct trajectories in schizophrenia. *Nature Mental Health*, *1*(3), 186–199. doi:10.1038/s44220-023-00024-0
- Kaloupek, A. V., & Nutt, D. J. (2007). Role of GABA in anxiety and depression. *Depression and Anxiety*, *24*(7), 495–517. doi:10.1002/da.20262
- Kaplanski, G. (2018). Interleukin-18: Biological properties and role in disease pathogenesis. *Immunological Reviews*, *281*(1), 138–153. doi:10.1111/imr.12616
- Kendler, K. S., & Gardner, C. O. Jr. (1998). Boundaries of major depression: An evaluation of DSM-IV criteria. *American Journal of Psychiatry*, *155*(2), 172–177. doi:10.1176/ajp.155.2.172
- Kessing, L., & Andersen, P. (2004). Does the risk of developing dementia increase with the number of episodes in patients with depressive disorder and in patients with bipolar disorder? *Journal of Neurology, Neurosurgery & Psychiatry*, *75*(12), 1662–1666. doi:10.1136/jnnp.2003.031773
- Krystal, J. H. (2014). Psychiatric disorders: Diagnosis to therapy. *Cell*, *157*(1), 201–214. doi:10.1016/j.cell.2014.02.042
- Kupfer, D. J., Frank, E., & Phillips, M. L. (2012). Major depressive disorder: New clinical, neurobiological, and treatment perspectives. *Lancet (London, England)*, *379*(9820), 1045–1055. doi:10.1016/S0140-6736(11)60602-8
- Lake, B. B., Chen, S., Sos, B. C., Fan, J., Kaeser, G. E., Yung, Y. C., ... Zhang, K. (2018). Integrative single-cell analysis of transcriptional and epigenetic states in the human adult brain. *Nature Biotechnology*, *36*(1), 70–80. doi:10.1038/nbt.4038
- Li, J., Seidlitz, J., Suckling, J., Fan, F., Ji, G.-J., Meng, Y., ... Chen, H. (2021). Cortical structural differences in major depressive disorder correlate with

- cell type-specific transcriptional signatures. *Nature Communications*, 12(1), 1–14. doi:10.1038/s41467-021-21943-5
- Li, M., Santpere, G., Imamura Kawasawa, Y., Evgrafov, O. V., Gulden, F. O., Pochareddy, S., ... Sestan, N. (2018). Integrative functional genomic analysis of human brain development and neuropsychiatric risks. *Science (New York, N.Y.)*, 362(6420), eaat7615. doi:10.1126/science.aat7615
- Lv, J., Di Biase, M., Cash, R. F., Cocchi, L., Cropley, V. L., Klausner, P., ... Cetin-Karayumak, S. (2021). Individual deviations from normative models of brain structure in a large cross-sectional schizophrenia cohort. *Molecular Psychiatry*, 26(7), 3512–3523. doi:10.1038/s41380-020-00882-5
- Marquand, A. F., Kia, S. M., Zabih, M., Wolfers, T., Buitelaar, J. K., & Beckmann, C. F. (2019). Conceptualizing mental disorders as deviations from normative functioning. *Molecular Psychiatry*, 24(10), 1415–1424. doi:10.1038/s41380-019-0441-1
- Marquand, A. F., Rezek, I., Buitelaar, J., & Beckmann, C. F. (2016). Understanding heterogeneity in clinical cohorts using normative models: Beyond case-control studies. *Biological Psychiatry*, 80(7), 552–561. doi:10.1016/j.biopsych.2015.12.023
- Meda, S. A., Clementz, B. A., Sweeney, J. A., Keshavan, M. S., Tamminga, C. A., Ivleva, E. I., & Pearlson, G. D. (2016). Examining functional resting-state connectivity in psychosis and its subgroups in the bipolar-schizophrenia network on intermediate phenotypes cohort. *Biological Psychiatry: Cognitive Neuroscience and Neuroimaging*, 1(6), 488–497. doi:10.1016/j.bpsc.2016.07.001
- Morgan, S. E., Seidlitz, J., Whitaker, K. J., Romero-Garcia, R., Clifton, N. E., Scarpazza, C., ... Donohoe, G. (2019). Cortical patterning of abnormal morphometric similarity in psychosis is associated with brain expression of schizophrenia-related genes. *Proceedings of the National Academy of Sciences of the United States of America*, 116(19), 9604–9609. doi:10.1073/pnas.1820754116
- O'Donovan, M. C., & Owen, M. J. (2016). The implications of the shared genetics of psychiatric disorders. *Nature Medicine*, 22(11), 1214–1219. doi:10.1038/nm.4196
- Pearlson, G. D., Clementz, B. A., Sweeney, J. A., Keshavan, M. S., & Tamminga, C. A. (2016). Does biology transcend the symptom-based boundaries of psychosis? *Psychiatric Clinics of North America*, 39(2), 165–174. doi:10.1016/j.psc.2016.01.001
- Peralta, V., & Cuesta, M. J. (1998). Lack of insight in mood disorders. *Journal of Affective Disorders*, 49(1), 55–58. doi:10.1016/s0165-0327(97)00198-5
- Peterson, M. J., & Benca, R. M. (2006). Sleep in mood disorders. *Psychiatric Clinics of North America*, 29(4), 1009–1032. doi:10.1016/j.psc.2006.09.003
- Pober, J. S., & Sessa, W. C. (2015). Inflammation and the blood microvascular system. *Cold Spring Harbor Perspectives in Biology*, 7(1), a016345. doi:10.1101/cshperspect.a016345
- Qiu, L., Lui, S., Kuang, W., Huang, X., Li, J., Zhang, J., ... Gong, Q. (2014). Regional increases of cortical thickness in untreated, first-episode major depressive disorder. *Translational Psychiatry*, 4(4), e378–e378. doi:10.1038/tp.2014.18
- Romero-Garcia, R., Seidlitz, J., Whitaker, K. J., Morgan, S. E., Fonagy, P., Dolan, R. J., ... Bullmore, E. (2020). Schizotypy-related magnetization of cortex in healthy adolescence is colocated with expression of schizophrenia-related genes. *Biological Psychiatry*, 88(3), 248–259. doi:10.1016/j.biopsych.2019.12.005
- Rydin, A. O., Milaneschi, Y., Quax, R., Li, J., Bosch, J. A., Schoevers, R. A., ... Lamers, F. (2023). A network analysis of depressive symptoms and metabolomics. *Psychological Medicine*, 53(15), 7385–7394. doi:10.1017/S0033291723001009
- Sarrazin, S., Cachia, A., Hozer, F., McDonald, C., Emsell, L., Cannon, D. M., ... Hamdani, N. (2018). Neurodevelopmental subtypes of bipolar disorder are related to cortical folding patterns: An international multicenter study. *Bipolar Disorders*, 20(8), 721–732. doi:10.1111/bdi.12664
- Seidlitz, J., Nadig, A., Liu, S., Bethlehem, R. A., Vertes, P. E., Morgan, S. E., ... Clasen, L. S. (2020). Transcriptomic and cellular decoding of regional brain vulnerability to neurogenetic disorders. *Nature Communications*, 11(1), 3358. doi:10.1038/s41467-020-17051-5
- Sheline, Y. I. (2003). Neuroimaging studies of mood disorder effects on the brain. *Biological Psychiatry*, 54(3), 338–352. doi:10.1016/s0006-3223(03)00347-0
- Sun, X., Sun, J., Lu, X., Dong, Q., Zhang, L., Wang, W., ... Wei, D. (2023). Mapping neurophysiological subtypes of major depressive disorder using normative models of the functional connectome. *Biological Psychiatry*, 94(12), 936–947. doi:10.1016/j.biopsych.2023.05.021
- Sweeney, M. D., Sagare, A. P., & Zlokovic, B. V. (2018). Blood–brain barrier breakdown in Alzheimer disease and other neurodegenerative disorders. *Nature Reviews Neurology*, 14(3), 133–150. doi:10.1038/nrneuro.2017.188
- Tonna, M., De Panfilis, C., & Marchesi, C. (2012). Mood-congruent and mood-incongruent psychotic symptoms in major depression: The role of severity and personality. *Journal of Affective Disorders*, 141(2–3), 464–468. doi:10.1016/j.jad.2012.03.017
- Voineskos, A. N., Mulsant, B. H., Dickie, E. W., Neufeld, N. H., Rothschild, A. J., Whyte, E. M., ... Lerch, J. P. (2020). Effects of antipsychotic medication on brain structure in patients with major depressive disorder and psychotic features: Neuroimaging findings in the context of a randomized placebo-controlled clinical trial. *JAMA Psychiatry*, 77(7), 674–683. doi:10.1001/jamapsychiatry.2020.0036
- Wei, Y., Womer, F. Y., Sun, K., Zhu, Y., Sun, D., Duan, J., ... Zhang, Y. (2023). Applying dimensional psychopathology: Transdiagnostic prediction of executive cognition using brain connectivity and inflammatory biomarkers. *Psychological Medicine*, 53(8), 3557–3567. doi:10.1017/S0033291722000174
- Wei, Y.-g., Duan, J., Womer, F. Y., Zhu, Y., Yin, Z., Cui, L., ... Jiang, X. (2020). Applying dimensional psychopathology: Transdiagnostic associations among regional homogeneity, leptin and depressive symptoms. *Translational Psychiatry*, 10(1), 248. doi:10.1038/s41398-020-00932-0
- Wen, J., Fu, C. H., Tosun, D., Veturi, Y., Yang, Z., Abdulkadir, A., ... Singh, A. (2022). Characterizing heterogeneity in neuroimaging, cognition, clinical symptoms, and genetics among patients with late-life depression. *JAMA Psychiatry*, 79(5), 464–474. doi:10.1001/jamapsychiatry.2022.0020
- Xia, M., Womer, F. Y., Chang, M., Zhu, Y., Zhou, Q., Edmiston, E. K., ... Xu, K. (2019). Shared and distinct functional architectures of brain networks across psychiatric disorders. *Schizophrenia Bulletin*, 45(2), 450–463. doi:10.1093/schbul/sby046
- Ye, H., Zalesky, A., Lv, J., Loi, S. M., Cetin-Karayumak, S., Rathi, Y., ... Di Biase, M. A. (2021). Network analysis of symptom comorbidity in schizophrenia: Relationship to illness course and brain white matter microstructure. *Schizophrenia Bulletin*, 47(4), 1156–1167. doi:10.1093/schbul/sbab015
- Zhang, W., Sweeney, J. A., Bishop, J. R., Gong, Q., & Lui, S. (2023). Biological subtyping of psychiatric syndromes as a pathway for advances in drug discovery and personalized medicine. *Nature Mental Health*, 1(2), 88–99. doi:10.1038/s44220-023-00019-x
- Zhang, X., Wang, F., & Zhang, W. (2022). Response to: Significance and stability of deep learning-based identification of subtypes within major psychiatric disorders. *Molecular Psychiatry* (2022). *Molecular Psychiatry*, 27(9), 3569–3570. doi:10.1038/s41380-022-01613-8
- Zhao, D., Wu, Z., Zhang, H., Mellor, D., Ding, L., Wu, H., ... Peng, D. (2018). Somatic symptoms vary in major depressive disorder in China. *Comprehensive Psychiatry*, 87, 32–37. doi:10.1016/j.comppsy.2018.08.013
- Zhou, Y., Zhou, B., Pache, L., Chang, M., Khodabakhshi, A. H., Tanaseichuk, O., ... Chanda, S. K. (2019). Metascape provides a biologist-oriented resource for the analysis of systems-level datasets. *Nature Communications*, 10(1), 1523. doi:10.1038/s41467-019-09234-6
- Zlokovic, B. V. (2011). Neurovascular pathways to neurodegeneration in Alzheimer's disease and other disorders. *Nature Reviews Neuroscience*, 12(12), 723–738. doi:10.1038/nrn3114
- Zong, X., Zhang, J., Li, L., Yao, T., Ma, S., Kang, L., ... Hu, M. (2023). Virtual histology of morphometric similarity network after risperidone monotherapy and imaging-epigenetic biomarkers for treatment response in first-episode schizophrenia. *Asian Journal of Psychiatry*, 80, 103406. doi:10.1016/j.ajp.2022.103406